Dissolved iron in the tropical and subtropical Atlantic Ocean

B. A. Bergquist[1,2] and E. A. Boyle[1]

Received 7 March 2005; revised 25 October 2005; accepted 28 November 2005; published 18 March 2006.

[1] Detailed depth profiles and surface transects of dissolved iron (DFe defined by 0.4-μm filtration) were investigated on three cruises in the subtropical and tropical Atlantic Ocean where dust deposition varied by 3 orders of magnitude. Surface DFe and dissolved Mn concentrations reflected dust deposition trends, but are not proportional to the estimated inputs. Using estimates of the atmospheric flux of DFe, surface DFe residence times were calculated to be on the order of 1 to 5 months. Deepwater DFe concentrations varied with water masses depending on their source, age, and transit pathways. At a site located on the edge of the equatorial system (10°N, 45°W), high DFe (>1 nmol/kg) was associated with an oxygen minimum zone at depths of 130 to 1100 m. DFe concentrations in North Atlantic Deep Water (NADW) decreased by 30% from sites in the North Atlantic to a site in the South Atlantic (24.5°S, 37°W), and DFe was lower in the Antarctic derived water masses (~0.4 nmol/kg) than in NADW at the South Atlantic site. An estimate of deepwater scavenging residence time for DFe was 270 ± 140 years based on decreasing DFe along the NADW flow path.

Citation: Bergquist, B. A., and E. A. Boyle (2006), Dissolved iron in the tropical and subtropical Atlantic Ocean, *Global Biogeochem. Cycles*, *20*, GB1015, doi:10.1029/2005GB002505.

1. Introduction

[2] Iron is an essential nutrient for all living organisms and, in particular, is necessary for chlorophyll production and nitrogen assimilation [*Rueter and Ades*, 1987]. Despite its abundance in the environment, the low solubility of Fe under oxidizing conditions results in very low dissolved Fe concentrations and Fe limitation of primary productivity in many of regions of the ocean [*Martin and Fitzwater*, 1988; *Martin*, 1990; *Martin et al.*, 1990a, 1994; *Coale et al.*, 1996; *Hutchins and Bruland*, 1998; *Boyd et al.*, 2000, 2004; *Coale et al.*, 2004]. This observation has lead to proposals that changes in Fe flux to the ocean may play a role in climate change by influencing primary production (and hence the carbon cycle) of the ocean [*Martin*, 1990; *Kumar et al.*, 1995; *Falkowski*, 1998]. In order to incorporate iron into models of climate change, it is necessary to understand and quantify the processes that control iron distributions in the ocean. There have been many attempts to model Fe in the ocean and to include Fe in models of atmospheric CO_2 and climate change [*Lefevre and Watson*, 1999; *Mahowald et al.*, 1999; *Archer and Johnson*, 2000; *Fung et al.*, 2000; *Sigman and Boyle*, 2000; *Gao et al.*, 2001; *Gregg et al.*, 2003; *Parekh et al.*, 2005]. However, it is difficult to constrain biogeochemical models for Fe because of the paucity of data throughout the ocean. New water column profiles of Fe, especially in areas not previously sampled, and new process studies of Fe biogeochemistry are necessary to improve and challenge our current understanding of Fe in the ocean.

[3] The main sources of Fe to the ocean are rivers, atmospheric deposition, resuspension of sediments, and hydrothermal vents. Fe concentrations are highest near its sources, and concentrations decrease rapidly with distance from sources due to the reactivity and insolubility of Fe in seawater [*Wu and Luther*, 1996; *Johnson et al.*, 1997]. Because Fe from rivers and resuspension of sediments from the coastal zone generally does not penetrate far into the ocean interior and hydrothermal Fe input is considered localized, it is believed that the main input of Fe to the open ocean is atmospheric deposition [*Duce and Tindale*, 1991; *Wells et al.*, 1995]. Scavenging onto particles and biological export followed by burial in sediments are generally thought to be the primary removal mechanisms. "Dissolved" iron (DFe: <0.4- or <0.2-μm filterable Fe) profiles in the open ocean are consistent with other nutrient-type elements showing depletion in the surface waters and an increase with depth owing to remineralization of organic matter [*Martin and Fitzwater*, 1988; *Bruland et al.*, 1994; *Johnson et al.*, 1997]. However, unlike many nutrient-type elements (e.g., P, N, Cd), DFe concentrations do not increase with increasing age of deep water (as would be expected if it were accumulated from remineralization of sinking organic matter) because of its particle-reactive behavior (like Al and Pb). In contrast to the concentrations of particle-reactive elements that are usually higher in the more continentally influenced Atlantic than the Pacific, deepwater Fe concentrations are low in both the Atlantic and Pacific, ~0.4 to 1 nmol/kg (for a review, see *Johnson et al.* [1997]).

[1]Earth, Atmospheric, and Planetary Sciences, Massachusetts Institute of Technology, Cambridge, Massachusetts, USA.
[2]Now at Department of Geological Sciences, University of Michigan, Ann Arbor, Michigan, USA.

0886-6236/06/2005GB002505

[4] There have been several attempts to explain and model the unique distribution of DFe in the ocean [*Johnson et al.*, 1997; *Lefevre and Watson*, 1999; *Archer and Johnson*, 2000; *Parekh et al.*, 2005]. The basic mechanisms of these models can be summarized as follows: (1) dissolution of atmospheric iron in surface waters, (2) biological uptake in the surface ocean, (3) transport to the deep ocean through biological export, (4) remineralization of organic material at depth releasing iron, (5) some solubilizing mechanism to keep iron in solution above inorganic solubility (e.g., organic complexation), and finally (6) scavenging and removal of iron. Earlier models assumed that organic ligands kept deep ocean DFe concentrations relatively constant (~0.6 to 0.7 nmol/kg) and only Fe in excess of the dissolved ligands was scavenged [*Johnson et al.*, 1997; *Lefevre and Watson*, 1999; *Archer and Johnson*, 2000]. However, the apparent constancy of the deepwater DFe in the ocean was over-emphasized in earlier data sets [*Boyle*, 1997]. There are areas of the open ocean where deepwater values deviate from the average ~0.6 to 0.7 nmol/kg value. DFe concentrations are lower (~0.4 nmol/kg) in the deep North Pacific [*Bruland et al.*, 1994; *Boyle et al.*, 2005] and also at 800 m in the Southern Ocean (0.2 to 0.3 nmol/kg) [*de Baar et al.*, 1999]. It is more likely that deepwater values of iron are controlled by a balance between input of dissolved iron in the deep water (both from remineralization and lateral transport) and removal by scavenging. Further, the organic ligand pool is usually in excess of DFe concentrations [*Gledhill and van den Berg*, 1994; *Rue and Bruland*, 1995; *Wu and Luther*, 1995; *Witter and Luther*, 1998; *Powell and Donat*, 2001]. Thus organic ligands likely enhance the residence time and solubility of DFe, but do not lead to uniform deep ocean values. The mechanism described above allows for more variable deepwater Fe concentrations.

[5] Besides assuming uniform deepwater DFe, Fe models typically use a constant percentage of dissolution for atmospheric aerosol Fe and constant Fe:C ratios for organic matter exported from the euphotic zone to the deep ocean. Model results are very sensitive to these parameters, and both of these assumptions have been challenged [*Sunda*, 1997; *Jickells and Spokes*, 2001; *Johnson et al.*, 2003; *Bergquist*, 2004; *Chen and Siefert*, 2004; *Boyle et al.*, 2005]. Another challenge to modeling iron is that large regions of the deep ocean have yet to be sampled, such as the Indian Ocean, the South Atlantic, the South Pacific, the Arctic, and high dust-flux regions of the North Atlantic. More data on the distribution of Fe and better constraints on parameters such as the residence time of Fe in both the upper and deep ocean, Fe:C ratios of exported organic matter from the euphotic zone, and atmospheric aerosol solubility are needed to improve our understanding and models of Fe behavior.

[6] Comparisons of Fe with other trace metals may be useful in understanding and quantifying certain aspects of the Fe cycle in the ocean especially in the surface ocean. In this study, Mn was measured and published Al data is available along a transect near our surface transect in the western Atlantic [*Vink and Measures*, 2001]. Mn and Al are also particle reactive and have distributions in the ocean that reflect their sources (aeolian deposition); however, unlike Fe, neither of these elements have profiles and distributions indicative of biological recycling [*Klinkhammer and Bender*, 1980; *Landing and Bruland*, 1980; *Orians and Bruland*, 1986; *Bruland et al.*, 1994]. Aluminum is considered an excellent tracer of atmospheric deposition in the surface ocean [*Measures and Brown*, 1996; *Measures and Vink*, 2000; *Vink and Measures*, 2001]. It has elevated surface concentrations and decreases with depth due to scavenging with a residence time of 3–5 years in the surface ocean [*Orians and Bruland*, 1986]. Manganese also has a surface maximum and decreases with depth, but surface values are higher than what would be predicted from atmospheric deposition and removal via scavenging. Photochemical cycling maintains higher concentrations and results in a longer residence time of $\leq$20 years in surface waters [*Landing and Bruland*, 1980, 1987; *Sunda and Huntsman*, 1988].

[7] The aim of this study was to investigate Fe distribution, speciation, and dissolution in areas of varying atmospheric dust inputs in the tropical and subtropical Atlantic Ocean. Iron concentrations were measured by a new isotope dilution multicollector inductively coupled plasma mass spectrometry (MC-ICPMS) method, which allows Mn and Cr concentrations to be measured simultaneously [*Bergquist*, 2004; *Boyle et al.*, 2005]. We present DFe and limited Mn data (DFe, DMn, <0.4 μm filtered) from three cruises in the subtropical and tropical Atlantic Ocean (30°N to 30°S) including both surface data and depth profiles of Fe.

2. Sampling and Methods

2.1. Sampling Sites

[8] Between January 2001 and March 2002, trace metal clean seawater samples were collected on three cruises in the subtropical and tropical Atlantic Ocean (Figure 1): (1) January 2001 (R/V *Seward Johnson*, SJ0101, surface sampling and deep profiles), (2) June/July 2001 (R/V *Knorr*, Knr162, surface sampling and detailed euphotic zone profiles), and (3) March 2002 (R/V *Endeavor*, En367, surface sampling, detailed euphotic zone and deep profiles). The two 2001 cruises that focused on the North Atlantic were part of the NSF-sponsored Biocomplexity MANTRA program in which sampling sites were chosen on the basis of variations in dust input. Two sites were visited in both the winter and summer of 2001 (30°N, 45°W and 10°N, 45°W), which allowed for sampling at both times of year in the upper 200 m. The northern site at 30°N is in the subtropical gyre and is characterized by oligotrophic conditions, a deep pycnocline, and lower atmospheric dust inputs than the 10°N site. The 10°N site is on the edge of the subtropical gyre and equatorial system, has a shallow pycnocline, and higher atmospheric dust inputs. The March 2002 cruise followed along the western part of the Atlantic basin from Barbados to Rio de Janeiro, Brazil. The deep South Atlantic profile presented in this study was taken at the southernmost extent of the cruise (24.5°S, 37°W) in the subtropical gyre of the South Atlantic.

[9] The sampling sites cover an area in the Atlantic Ocean where estimated dust deposition fluxes vary by orders of

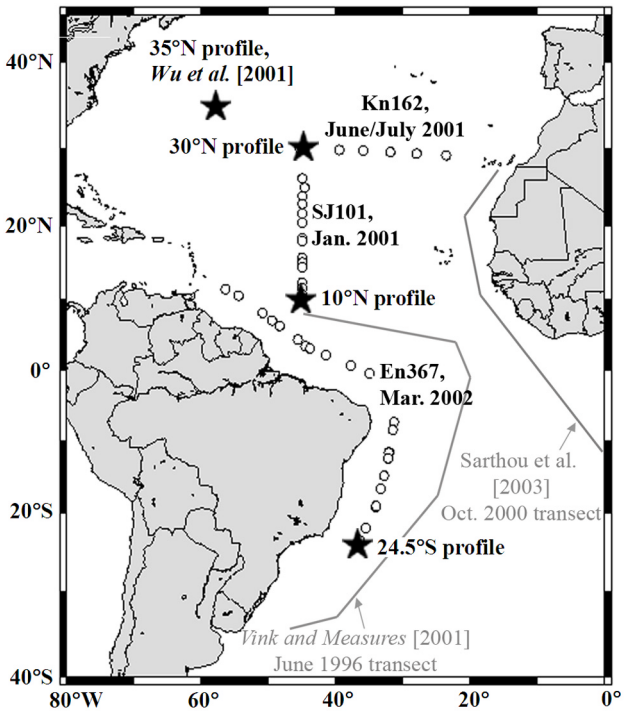

Figure 1. Sample location map for the three cruises discussed in this study. Surface samples analyzed in this study are marked by circles, and profile sites are marked by stars. Published sampling locations and transects used for comparison are also shown.

magnitude both from north to south and seasonally [*Duce and Tindale*, 1991; *Fung et al.*, 2000; *Gao et al.*, 2001; *Vink and Measures*, 2001; *Chen and Siefert*, 2004]. Dust deposition rates are highest in the North Atlantic downwind from the Sahara and decrease rapidly south of the intertropical convergence zone (ITZC). Generally, dust fluxes to the tropical and subtropical Atlantic are estimated to be highest in the Northern Hemisphere summer [*Prospero*, 1996; *Gao et al.*, 2001]. However, seasonally high winter atmospheric dust concentrations have been observed in the eastern tropical Atlantic in the zone of maximum dust transport off the Sahara [*Chiapello et al.*, 1995]. On the North Atlantic cruises, particulate and labile Fe (90-min, pH 4.5, reducing leach) atmospheric concentrations were measured concurrently at sea [*Chen and Siefert*, 2004].

2.2. Sampling Methods

[10] The trace metal clean seawater samples collected in this study were collected using a variety of methods. Many of the samples collected on the cruise were taken with the Moored In situ Trace Element Serial Sampler (MITESS) water sampler or with a single MITESS "ATE" (Automated Trace Element) module [*Bell et al.*, 2002]. Each MITESS module opens and closes an acid-cleaned 500-mL polyethylene bottle while underwater in order to minimize chances for contamination. Details of the different types of sampling schemes are given by *Bergquist* [2004] and *Boyle et al.* [2005]. For profile work, it is especially challenging to collect trace metal clean samples in the upper 30 m of the water column while maintaining good depth control. Details of the upper water column sampling can be found in online auxiliary material[1]. After sample collection, sealed sample bottles were taken into a class 100 clean air flow environment for filtration within 12–24 hours of collection in order to avoid Fe loss to bottle walls. Multiple splits of each sample were vacuum filtered through acid cleaned 0.4-μm Nuclepore® filters. Filtrates were acidified at sea to pH 2 by addition of triply distilled Vycor 6 N HCl in a ratio of 1 mL acid to 500 mL of seawater.

2.3. Fe and Mn Measurement

[11] Iron, Mn, and Cr concentrations in filtrates were measured simultaneously by a modified version of the method by *Wu and Boyle* [1998], which utilizes isotope dilution followed by $Mg(OH)_2$ coprecipitation and measurement by ICPMS [*Bergquist*, 2004; *Boyle et al.*, 2005]. This paper focuses on the Fe data with limited Mn data (details of method and the data are available in Text S1 and Tables S1 and S2 in the auxiliary material). Additional details of the method and the Mn and Cr data are given by *Bergquist* [2004]. Briefly, the main differences of the new method used in this study are the use of a ^{54}Fe isotope spike and a GV Instruments IsoProbe MC-ICPMS. The IsoProbe incorporates a hexapole collision cell prior to the magnet that eliminates $^{40}Ar^{16}O^+$ and $^{40}Ar^{14}N^+$ interferences on masses 56 and 54, which allows samples to be measured in low mass resolution. The multi-collection feature permits simultaneous collection of masses 52 (monitor Cr and correct for Cr interference on 54), 54, 55 (Mn), 56, and 57. The largest interference correction for Fe is CaO^+ on mass 56. The CaO^+ interference is monitored by measuring $CaOH^+$ on mass 57, measuring the CaO/CaOH ratio on a trace metal clean Ca solution throughout the run, and correcting mass 56 for the CaO^+ interference. Mn and Cr concentrations are calculated by measuring recovery efficiency (from spiked samples) compared to the ^{54}Fe spike and by measuring the relative ionization efficiencies of Mn, Cr, and Fe in the plasma.

[12] Replicate analysis of samples yield precisions of better than ±0.05 nmol/kg for Fe and ±0.15 nmol/kg for Mn. Error bars reported in this study represent the 1σ standard deviation of replicate analysis of samples. Procedural blanks for Fe ranged from 0.08 to 0.17 nmol/kg for individual analysis sessions with typical precisions of ±0.03 nmol/kg (1σ SD) for individual sessions. For Mn, procedural blanks ranged from 0.4 to 1.0 nmol/kg with typical precisions of ±0.1 nmol/kg (1σ SD) for individual runs. We feel differences between samples in our extended data set are comparable to within the analytical session sample replication (±0.05 nmol/kg (1SD) for Fe). Comparisons of our data to other published data sets within ~0.15 nmol/kg for Fe should be made with caution, as no interlaboratory consistency sample was available at the time these measurements were made. However, agreement (within 0.05 nmol/kg) between deepwater concentrations in DFe in the North Pacific measured in our lab [*Boyle et al.*, 2005] and concentrations observed at a nearby station

[1]Auxiliary material is available at ftp://ftp.agu.org/apend/gb/2005gb002505.

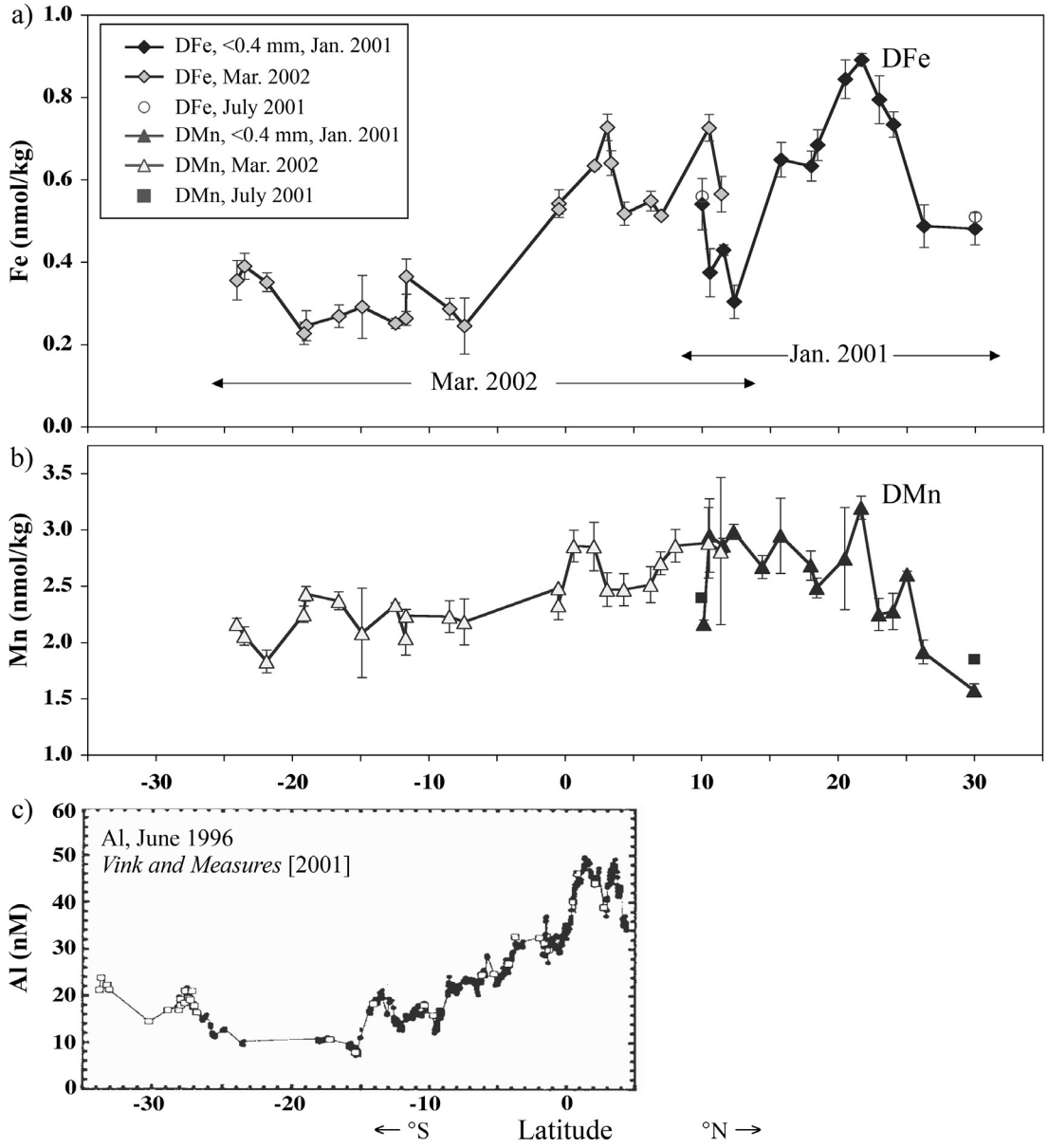

Figure 2. (a) DFe surface data along a N-S transect from 30°N to 25°S in the western Atlantic (transects from the January 2001 and March 2002 cruises were combined). DFe data for the stations resampled on the summer 2001 cruise are also shown (30°N and 10°N). (b) DMn data from the same surface samples as in Figure 2a. (c) Surface dissolved Al data from June 1996 along a similar transect in the western Atlantic from *Vink and Measures* [2001]. Error bars are 1σ standard deviation of sample replicates (external reproducibility is typically less than ±0.05 nmol/kg (1 SD) for DFe and less than ±0.15 nmol/kg for DMn).

by *Bruland et al.* [1994] suggests our method agrees well with other methods and laboratories.

3. Results and Discussion

3.1. Surface Water Fe and Mn Variability and Distribution

[13] The N-S surface distributions of DFe and DMn from 30°N to 25°S in the western Atlantic are shown in Figure 2 along with published dissolved Al data from a similar transect from June 1996 [*Vink and Measures*, 2001]. The N-S transects from the January 2001 (north section) and the March 2002 (south section) cruises were combined to make the figure. Although the two transects are a year apart and are from slightly different times of the year, the DFe values are similar where the transects overlap. DFe values are highest in the North Atlantic (0.60 ± 0.15 nmol/kg, 1 SD, n = 23) and decrease by a factor of 2 south of 0.5°S (0.30 ± 0.06 nmol/kg, 1 SD, n = 12). A maximum in DFe is seen at 20°N with a peak value of 0.89 nmol/kg. *Sarthou et al.* [2003] also observed

higher DFe (0.40 nmol/kg) in the North Atlantic and lower concentrations in the South Atlantic (0.11 nmol/kg) in the eastern Atlantic in October 2000 (transect shown in Figure 1).

[14] The observed pattern in the surface DFe is similar to trends of other dust derived trace metals (e.g., Mn and Al) indicating that surface DFe reflects variations in dust input along the transect. DMn measured along the same transect shows a similar pattern with average values of 2.60 ± 0.36 nmol/kg (1 SD, n = 26) in the North Atlantic and 2.19 ± 0.16 nmol/kg (1 SD, n = 12) in the South Atlantic. A broader maximum is observed for Mn between 0 and 25°N with a peak value of 3.2 nmol/kg. Dissolved Al data along a similar transect from *Vink and Measures* [2001] also shows higher values in the North Atlantic (40–50 nmol/kg) and a decrease in the South Atlantic to concentrations <10 nmol/kg in the subtropical gyre (Figure 2c). However, dissolved Al values decreased by more than a factor of 5 between the North and South Atlantic. DFe values decrease only by a factor of 2 and DMn decreases ~20%. For DFe, factors such as biological uptake, biological export, and scavenging result in a shorter residence time of less than a year in the surface ocean (as estimated in section 3.3.2) compared with Al (3–5 years). Solubility limits may also play a role in surface DFe profiles [*Vink and Measures*, 2001; *Wu and Boyle*, 2002]. If a proportional amount of Fe to Al was dissolved from atmospheric particles based on the composition of continental crust (8.0% Al, 4.3% Fe [*Wedepohl*, 1995]), one would expect higher DFe concentrations (20–25 nmol/kg) in the North Atlantic. Therefore the short residence time of Fe in surface waters and possible solubility limits lead to DFe values that are more variable than Al and that do not scale proportionally to Al in the North Atlantic. As for Mn, photochemical cycling leads to a longer surface residence time (≤20 years) than Al [*Landing and Bruland*, 1980; *Sunda and Huntsman*, 1988]. Thus enhanced cycling and lateral transport erase large flux variations.

[15] Both our DFe and DMn transect data show maxima in the North Atlantic near 20°N, which is consistent with this being the zone of maximum dust transport from the Sahara in the Northern Hemisphere summer months when dust fluxes are typically higher [*Husar et al.*, 1997; *Moulin et al.*, 1997]. The maximum at 20°N is in agreement with modeled surface DFe fluxes and concentrations [*Fung et al.*, 2000; *Gregg et al.*, 2003; *Parekh et al.*, 2005]. Surface DFe distributions were modeled seasonally by *Gregg et al.* [2003], although only an atmospheric Fe flux to surface water was included (no upwelling flux). The model produced the general pattern observed in the measured DFe of higher concentrations in the North Atlantic under the Saharan dust plume and the decrease of DFe to much lower concentrations (0.2 to 0.3 nmol/kg) in the subtropical gyre of the South Atlantic. However, the model-derived DFe concentrations in the region of the Saharan dust plume are higher (>1 nmol/kg) and the region of high DFe broader than our measured DFe in this region. Differences between the modeled and measured DFe are likely due to model assumptions (e.g., constant percentage of dust dissolution or constant scavenging rates), but the agreement for the general pattern of DFe indicates that 3-D general circulation models including dust dissolution, scavenging, and biological uptake for Fe are capturing many of the processes controlling surface DFe in this region of the ocean. Part of the agreement between modeled DFe and observed DFe in the Atlantic may be due to the dominance of the atmospheric flux component of DFe over the upwelling flux in the Atlantic subtropical and tropical surface ocean [*Fung et al.*, 2000]. In other regions where dust deposition is lower, models with an upwelling flux will be needed to better estimate the DFe in surface waters [*Parekh et al.*, 2005].

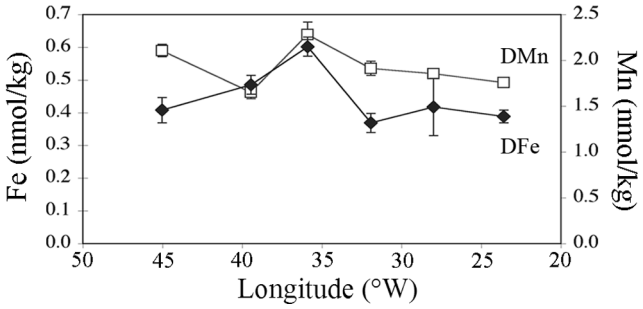

Figure 3. DFe and DMn along an E-W transect at ~30°N in the North Atlantic from the June/July 2001 cruise. Error bars are 1σ standard deviation of sample replicates (external reproducibility is typically less than ±0.05 nmol/kg (1 SD) for DFe and less than ±0.15 nmol/kg for DMn).

[16] Seasonal variability of surface DFe was not observed for the two stations (30°N and 10°N) sampled both in winter and summer of 2001. The 30°N station had a peak surface DFe of 0.68 nmol/kg in the winter and 0.50 nmol/kg in the summer. However, the peak value at 30°N in the winter is part of a well-defined surface maximum (see profiles in Figure 4a in section 3.3). The integrated mixed layer value for this station was 0.51 nmol/kg. Therefore the winter and summer surface DFe are similar at this site. Large differences in the DFe from winter to summer are also not observed at the higher dust site, 10°N, with winter surface DFe at 0.59 nmol/kg and summer at 0.56 nmol/kg. In contrast, in situ atmospheric dust measurements did show seasonal differences. *Chen and Siefert* [2004] measured total dust, total Fe, and labile Fe (90 min, pH = 4.5, reducing leach) concentrations in the atmosphere concurrently with our DFe. At the 10°N station, total and labile atmospheric Fe flux estimates are 5 times higher in the winter than in the summer. At the 30°N station, concurrent dust measurements are 5 times higher in the summer than in the winter. The poor correlation of our sea surface DFe concentrations and the concurrent dust flux estimates demonstrates the problem of trying to compare in situ atmospheric measurements with sea-surface DFe measurements. DFe integrates over weeks to months of dust deposition events and is biologically cycled with possible solubility controls. Dust deposition measurements at sea are made daily and may not represent the regional or seasonal input because of the episodic and spatially inhomogeneous nature of dust events [*Prospero*, 1996; *Jickells and Spokes*, 2001].

[17] DFe and DMn remain relatively invariant on an E-W transect (23°W to 45°W) along 30°N from the July 2001 cruise (Figure 3). Strong E-W gradients in dust deposition

or DFe at 30°N are also not predicted by models except for very high values close to the African continent where most of the larger particles are deposited [*Mahowald et al.*, 1999; *Fung et al.*, 2000; *Gregg et al.*, 2003]. *Sarthou et al.* [2003] measured surface DFe of greater than 1 nmol/kg closer to the African continent at 15°W. Our easternmost sample is at 23.6°W and had a DFe concentration of 0.40 nmol/kg suggesting that a steep longitudinal gradient may exist between these locations. Generally, our E-W data suggests that finer particles transported to the west of ~20°W are not preferentially deposited with longitude.

3.2. Surface Aerosol Solubility

[18] On the summer 2001 cruise, trace metal clean incubation experiments were performed by D. Capone and coworkers (University of Southern California) in order to investigate the effects of aerosol additions on phytoplankton growth at both the 10°N and 30°N stations. The mesocosm experiments were done in large carboys (20 L) in incubation chambers on deck. Atmospheric dust was collected for several days on large volume acid-cleaned filters (by R. Siefert and Y. Chen), and the filters sectioned and added to the mesocosm experiments. The mesocosm experiments were then allowed to incubate for varying amounts of time (0 to 5 days) and sampled by our group for DFe. Y. Chen and R. Siefert (personal communication, 2003) estimated that each section of dust filter had approximately 100 μg and 900 μg total Fe at the 30°N and 10°N stations, respectively.

[19] Release of excess DFe (the amount of DFe in excess of the ambient DFe of the natural seawater) from the aerosol filter additions was only observed at the 10°N station for the two 5-day incubation experiments. The experiments reached total concentrations of ~1.15 nmol/kg with an excess DFe of ~0.50 nmol/kg. Although a large amount of aerosol Fe was added to these experiments (900 μg), the proportion of this Fe released into the dissolved pool was very small (<0.1%). The upper concentration reached in these experiments may represent the saturation of organic ligands in the dissolved pool. Excess dissolved organic ligand concentrations were measured by *Wu and Luther* [1995] and *Luther and Wu* [1997] in surface water of the northwestern Atlantic Ocean. Excess ligand concentrations of $0.45 - 0.60 \pm 0.20$ nM were observed, which agrees well with our observed excess DFe for the 5-day mesocosm experiments. In contrast, the 30°N station experiments and the 3-day incubation experiment at 10°N had no detectable amounts of excess DFe released from the dust filters. It is unclear why no excess DFe was observed in these dust addition experiments. Dust concentrations were much lower at the 30°N station, and perhaps there is a kinetic barrier to dissolving Fe off the dust filters. Additionally if only a small amount of excess DFe were released, it could be quickly taken up by organisms or scavenged onto particles in the mesocosm experiments.

3.3. Fe Water Column Profiles

[20] Figures 4 through 7 show water column profiles of DFe at three sites along the N-S transect: (1) 30°N, 45°W, (2) 10°N, 45°W, and (3) 24.5°S, 36°W (Figure 1). A DFe profile from a station near the Bermuda Rise (35°N, 58°W) from *Wu et al.* [2001] is shown for comparison in Figure 6. The 30°N and 10°N stations were sampled both on the January and the July cruises. Deepwater profiles were collected in the winter (Figures 4a and 4c) and high-density euphotic zone profiles collected in the summer (Figures 4b and 4d). The goal of the high-density euphotic zone sampling was to examine Fe in this active zone in more detail. The South Atlantic site was sampled on the March 2002 cruise (Figures 5a and 5b). Table 1 summarizes the data from these profiles.

[21] The DFe concentration profiles generally have nutrient-type profiles with lower concentrations in surface waters than in deep water, although the profiles have interesting features deviating from classic nutrient-type profiles with surface maxima, intermediate water minima and maxima, and variations clearly associated with water masses. Profiles will be discussed in terms of their upper and deepwater column profiles. Residence time calculations were made for surface Fe where steady-state assumptions could be made and also for deepwater Fe.

3.3.1. Upper (Surface to ~1000 m) Water Column Fe Profiles

[22] The two subtropical gyre sites (30°N and 24.5°S) along with the subtropical gyre profile from *Wu et al.* [2001] near Bermuda have very different upper water column profiles of DFe compared to the 10°N site (Figures 4 through 7). The pycnocline extends deeper at the gyre sites (~750 m), whereas the pycnocline at 10°N is much shallower (<250 m). At all three gyre sites, surface maxima in DFe are observed followed by broad minima in the pycnocline before DFe increases below depths greater than 600 m (Figure 6a). At the 10°N station (on the edge of the equatorial system), a surface maximum in DFe is observed in the summer and not in the winter (Figures 4c and 4d). DFe values increase dramatically at this site to values >1 nmol/kg below the mixed layer and remain high to a depth of 1050 m (Figures 4c and 7.

[23] At all sites except 10°N in the winter, DFe had a surface maximum and decreased to low concentrations between 30 and 70 m. Below the depth where DFe minima occur, DFe concentrations remain low in the deep pycnoclines of the subtropical gyre sites (30°N and 24.5°S, Figure 6a). The winter surface maximum in DFe at 30°N station is higher (0.68 nmol/kg) than would be expected on the basis of very low atmospheric dust concentrations measured concurrently at the station [*Chen and Siefert*, 2004]. The DFe peak is very well defined within the mixed layer suggesting that the feature is transient and may be due to a dust deposition event prior to our sampling.

[24] The surface maxima in DFe are likely due to atmospheric deposition, but the reason for the decrease in DFe at shallow depths is less clear. There are two possible explanations for the decrease in DFe: (1) some removal mechanism for the DFe between ~30 to 80 m (i.e., scavenging and biological uptake), and/or (2) transient atmospheric dust deposition and downward mixing with lower DFe water. The minima in DFe are often associated with the chlorophyll maximum, which suggests that some biological uptake mechanism or scavenging at this depth may be responsible for the minima (Figure 4d). However, at the

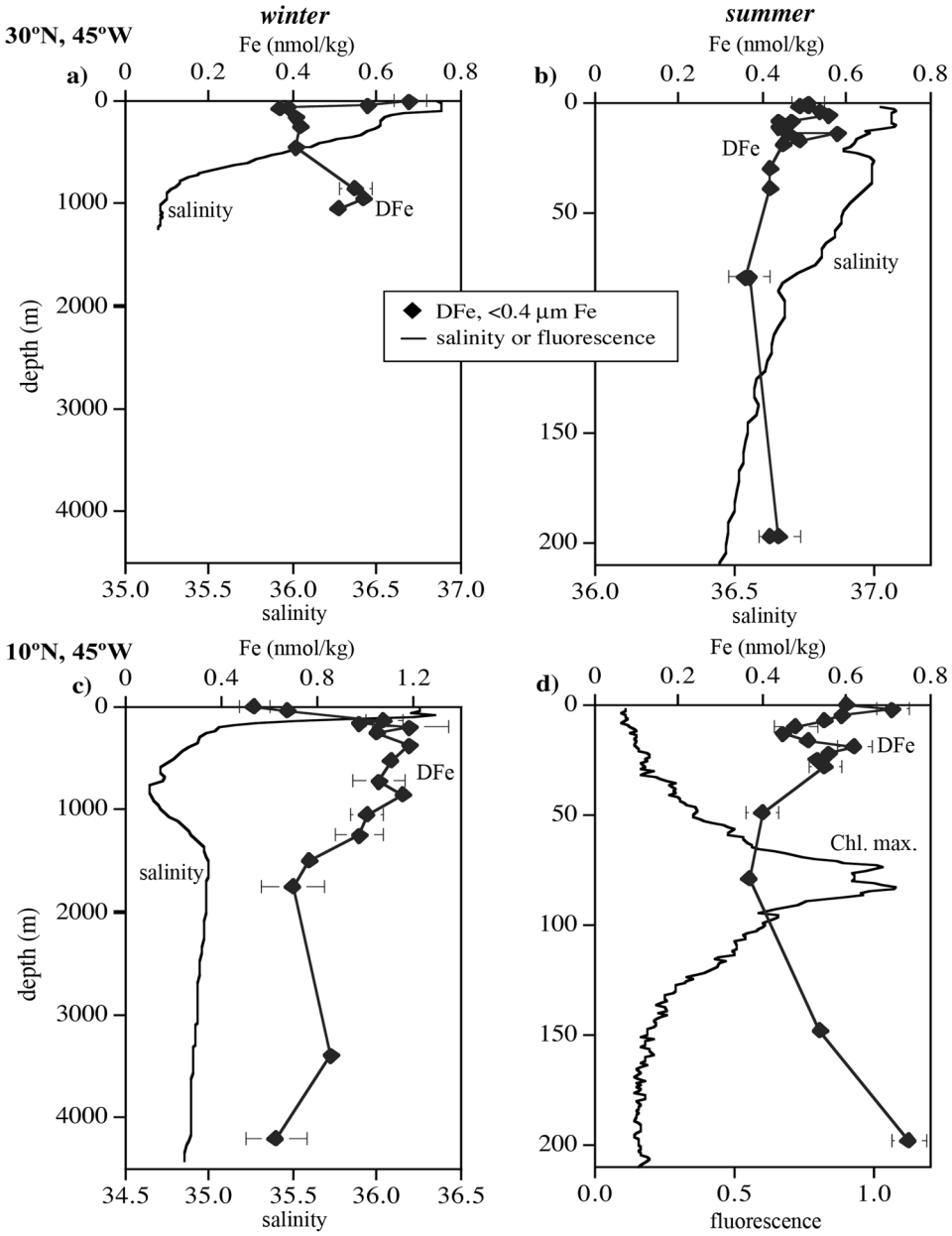

Figure 4. DFe water column data at the 30°N, 45°W and 10°N, 45°W stations from both the winter and summer cruises, 2001. (a) The winter 30°N station plotted with salinity. (b) The summer 30°N station plotted with salinity. (c) The winter 10°N station plotted with salinity. (d) The summer 10°N station plotted with chlorophyll fluorescence. Error bars are 1σ standard deviation of sample replicates (external reproducibility is typically less than ±0.05 nmol/kg (1 SD) for DFe).

subtropical gyre sites, DFe does not increase below the chlorophyll maximum within the pycnoclines as might be expected due to remineralization of organic matter based on major nutrient data. It could be that remineralization for Fe happens deeper and that the DFe is lower in the pycnocline water owing to the water source. The pycnocline water in the subtropical gyres is formed at higher latitudes (40°N) in the gyres and spreads along isopycnals [*Tchernia*, 1980]. This higher latitude source water is generally characterized by lower dust deposition and hence lower surface DFe. In particular in the South Atlantic, this water forms in an area of very low dust deposition. Therefore the pycnocline waters at the 24.5°S station are probably ventilated by water that sinks with very low DFe. The mechanism for the DFe minima in the deep pycnoclines of the subtropical gyre sites is not clear, but is likely a combination of the mechanisms listed above (scavenging/biological uptake and ventilation of the pycnocline with high latitude, low DFe water).

[25] The station at 10°N is different from the gyre stations in that the pycnocline is very shallow and high levels of

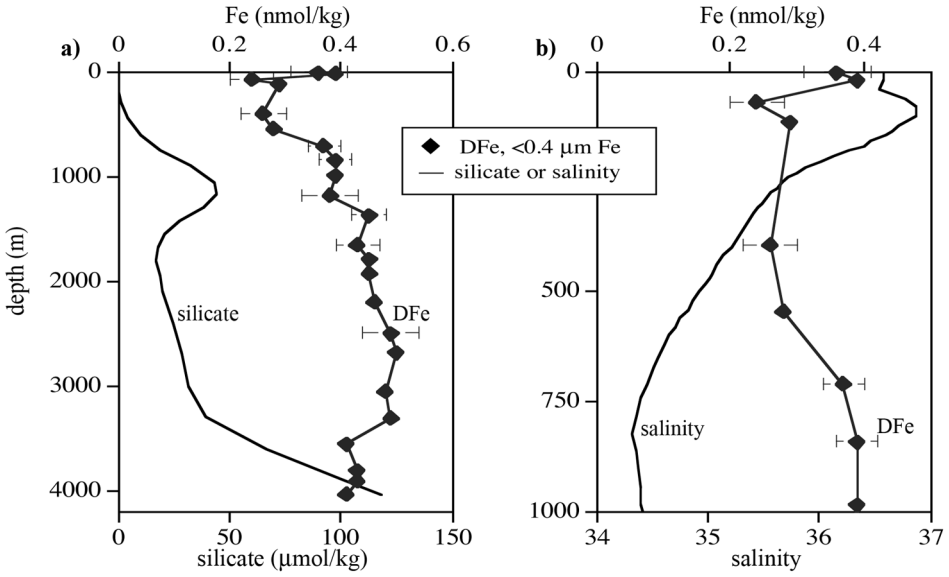

Figure 5. DFe profile for the South Atlantic station at 24.5°S, 37°W, which was occupied in March 2002. (a) The full DFe profile to 4500 m plotted along with reactive silicate data measured on the same cruise. (b) A magnification of the upper 1000 m plotted along with CTD salinity data. Error bars are 1σ standard deviation of sample replicates (external reproducibility typically less than ±0.05 nmol/kg (1 SD) for DFe).

DFe are observed in the upper 1000 m. The zone of high Fe concentration persists from 130 to 1050 m with an average DFe of 1.09 ± 0.08 nmol/kg (1 SD, n = 9). In the more stratified summer, a surface maxima in DFe exists followed by a shallow minima at 50 to 100 m. The same station in the winter was characterized by a deeper mixed layer, and the DFe concentration increased with depth with no observed minimum. A DFe minimum may not have occurred at this time of year due to winter vertical mixing with deeper high DFe water. DFe values increased to higher concentrations at shallower depths in the winter than in the summer.

[26] The Fe maximum at 10°N from 130 to 1050 m is associated with an oxygen minimum zone (OMZ) (Figure 7). The OMZ in the tropical Atlantic is due to enhanced

Table 1. Summary of Water Column Data

Station	Depth, m	DFe, nmol/kg	DFE, 1 SD[a]	n[b]	Fe*,[c] nmol/kg	Fe*, 1 SD[a]	AOU Calc. Fe:C,[d] μmol/mol	Fe:C, 1 SD[a]
35°N, 58°W	mixed layer, <20 m	0.57		1				
[*Wu et al.*, 2001]	pycnocline, 50–500 m	0.24	0.05	6				
	deep, >1500 m	0.64	0.05	6	0.04	0.07		
30°N, 45°W	winter mixed, 0–100 m	0.51	0.15	4				
	winter mixed layer peak, 0 m	0.68		1				
	summer mixed layer. 0–11 m	0.50	0.05	8				
	pycnocline, 165–525 m	0.41	0.02	3				
	deep, 850–1050 m	0.54	0.03	3				
10°N, 45°W	winter mixed layer, 0–55 m	0.59	0.13	2				
	summer mixed layer, 0–32 m	0.56	0.07	11				
	O2 minimum, 150–1050 m	1.09	0.08	9	0.17	0.15	11	1
	deep, 1600–4200 m	0.73	0.12	3	0.13	0.12	17	3
24.5°S, 36°W	mixed layer, 0–52 m	0.37	0.03	2				
	pycnocline, 60–550 m	0.27	0.02	4				
	AAIW, 700–1200 m	0.38	0.01	4	−0.57	0.09	5.4	0.8
	NADW, 1700–3350 m	0.47	0.02	7	−0.15	0.02	11	1
	AABW/ACDW, >3500 m	0.42	0.01	4	−0.43	0.1	6.7	0.9

[a]Here 1 SD denotes 1σ standard deviation of depths used in sample grouping (not the same as analysis replicates).
[b]Here n denotes the number of depths used in sample grouping.
[c]Fe* is defined by *Parekh et al.* [2005] and is calculated from the following formula: [DFe] – [PO4−]*(Fe/P)uptake ratio. Phosphate data from nearby GEOSECS stations 39 and 57 were used for the 10°N and 24.5°S stations, respectively. For the *Wu et al.* [2001] station, Bermuda time series phosphate data were used from the winter of 2001. A biological uptake Fe:P ratio of 0.47 mmol/mol was used.
[d]Fe:C ratios were calculated using the measured AOU from nearby GEOSECS stations (above) and an organic remineralization O2:C ratio of −1.6 (similar to *Sunda* [1997]).

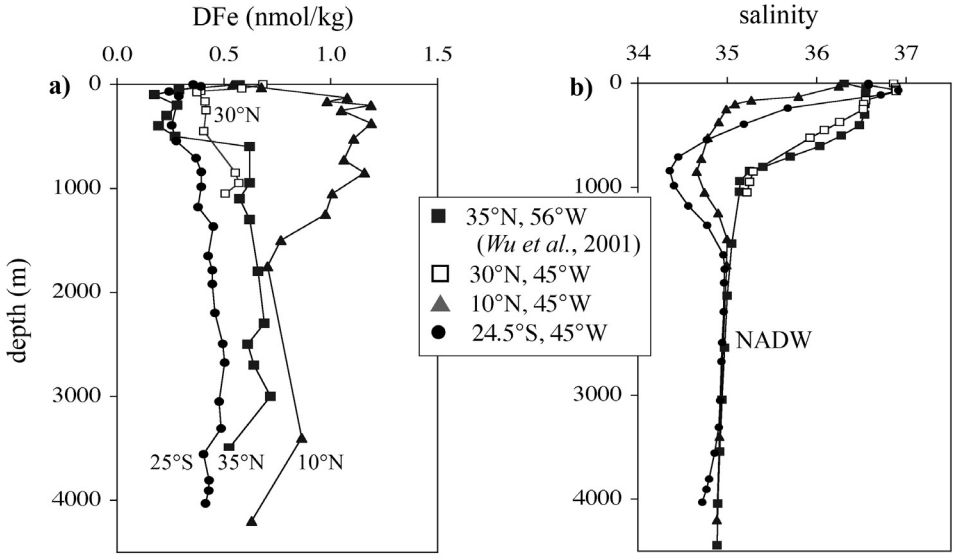

Figure 6. Fe water column data for the three deep stations sampled in this study (30°N, 45°W; 10°N, 45°W; 24.5°N, 36°W) along with a station sampled near the Bermuda Rise from *Wu et al.* [2001] (35°N, 56°W). (a) The DFe (<0.4 μm Fe) profiles. (b) The salinity profiles. In Figure 6b, the core of North Atlantic Deep Water (NADW) is marked.

remineralization of organic matter sinking from the high productivity equatorial and upwelling region off Northwest Africa and slow ventilation of the mid-depth water in this region (S. C. Doney, personal communication, 2004). The oxygen depletion below the euphotic zone to intermediate depth is strongest in the eastern basin and becomes weaker westward [*Fukumori et al.*, 1991]. The high Fe concentrations in the upper 1000 m at the 10°N site is likely from remineralization of organic matter sinking from the high-productivity equatorial region and accumulated organic matter remineralization in this slowly ventilated water mass. Higher DFe concentrations (on the order of 2 nmol/kg) in the OMZ have been observed for the eastern tropical Atlantic where oxygen concentrations are lower than at our site [*Landing et al.*, 2003].

[27] One can calculate an estimate of the Fe:C ratio for the remineralized organic matter in the oxygen minimum zone using the same method as *Sunda* [1997]. An Fe:C regeneration ratio of 11 ± 1 μmol/mol was calculated using the DFe concentrations, apparent oxygen utilization (AOU) from GEOSECS station 39 (8°N, 44°W), and an O_2:C ratio of −1.6 [*Martin et al.*, 1987]. Our ratio falls within the range of Fe:C regeneration ratios estimated by *Sunda* [1997] for the North Atlantic (7 to 12 μmol/mol) calculated using the *Johnson et al.* [1997] data compilation. The North Atlantic estimates of Fe:C regeneration ratios are higher than values for the Pacific or Southern Ocean regions (usually <6 μmol/mol). *Sunda* [1997] interpreted this difference to indicate that the organic matter sinking in the North Atlantic may have elevated Fe:C ratios compared with most of the ocean owing to the higher surface DFe and luxury Fe uptake by organisms [*Sunda and Huntsman*, 1995]. This AOU-derived Fe:C regeneration ratio could be overestimating the Fe:C ratio of exported organic matter if the water had preformed DFe (meaning it sank with a significant amount of DFe) or underestimating the ratio if significant scavenging of Fe has occurred in the water mass.

3.3.2. Surface Residence Time Estimates

[28] Surface residence time calculations were made at the profile sites for which reasonable assumptions of steady-

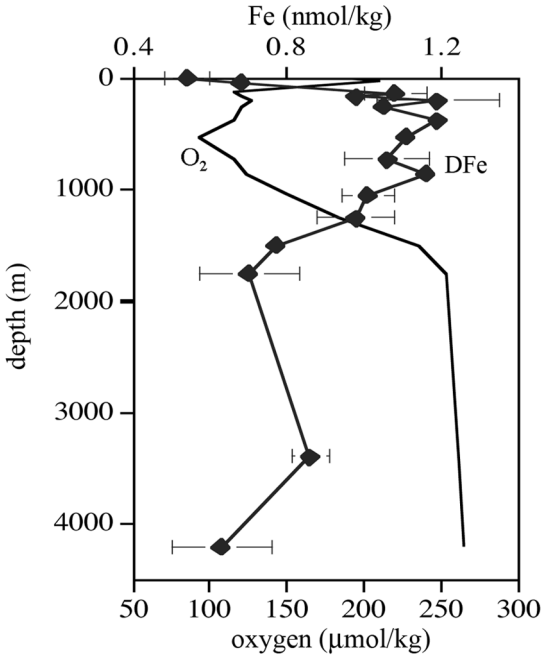

Figure 7. DFe from the winter 10°N, 45°W station plotted with dissolved oxygen data from the nearby GEOSECS station 39 (7.8°N, 43.9°W). Temperature and salinity overlays for our station and the GEOSECS station were nearly identical.

Table 2. Surface Residence Time Calculations[a]

Site	Mixed Layer Depth, m	Total Fe Flux, μg/m^2/d	Total Fe Flux, 1 SD	Percent Labile Fe	Total Labile Fe Flux, μg/m^2/d	Total Labile Fe Flux, 1 SD	Integrated DFe in Mixed Layer,[b] μg	Residence Time, days	Integrated DFe in Mixed Layer, 1 SD
10°N winter	55	630[c]	350[c]	5%	30[c]	16[d]	2055	69	37
10°N summer	32	278[c]	171[d]	2%	6.1[c]	3.3[d]	1000	164	89
30°N summer	11	203[c]	122[d]	3%	6.9[c]	5[d]	318	46	32
30°N winter	100	2.5[c]	1.4[d]	28%	0.7[c]	0.5[d]	2937	4196[e]	2997
24.5°S (varying dissolution)	52	88[f]		3%	2.7[g]	1.7[h]	1122	424	297
	52	88[f]		10%	8.8e	6.2[h]	1122	128	89

[a]Residence time estimates assume steady state and that atmospheric deposition is the only input flux into the system. Estimates do not consider vertical mixing or advection.

[b]This denotes integrated DFe in a 1 m^2 by the depth of mixed layer volume (calculated using measured DFe concentrations in the mixed layer).

[c]Total atmospheric Fe and labile Fe concentrations were measured concurrently at sea [*Chen and Siefert*, 2004]. Labile Fe was the Fe dissolved in a 90-min, reducing, pH 4.5 leaching solution. Fluxes were estimated assuming a 1 cm d^{-1} deposition rate.

[d]Standard deviation estimates from *Chen and Siefert* [2004] are the 1σ variability of many stations within each region.

[e]The 30°N had a surface maximum in the mixed layer and decreasing values of Fe in the mixed layer. The in situ measured dust flux for this region is too low to explain the Fe maximum and/or the steady state assumption for the DFe is incorrect. Thus residence time calculations for this station are likely unrealistically long.

[f]This is based on an estimate of dust flux for this region from June 1996 [*Vink and Measures*, 2001]. Total Fe deposition flux was calculated assuming an average continental crustal abundance for Fe of 4.3%.

[g]Since no estimate of total labile Fe exists for this station, two percent dust dissolution values were chosen based on observed labile Fe values from the North Atlantic data of *Chen and Siefert* [2004]; 3% is approximately the average and 10% is near the high end of observed fractions of labile Fe.

[h]Standard deviation is estimated from the typical variability of Fe flux observed in the work by *Chen and Siefert* [2004].

state could be made (Table 2). DFe concentrations were integrated over the depth of the mixed layer, and concurrent labile Fe deposition estimates (90-min, pH 4.5, reducing leach) were used as an input flux of DFe where available [*Chen and Siefert*, 2004]. This method assumes that atmospheric deposition is the dominant source of DFe to the mixed layer, that the labile Fe flux estimates are representative of the atmospheric input, and the DFe concentrations are at steady state. Excluding the winter 30°N site, estimates of surface residence times in the North Atlantic were 1.5 to 5 months (±50%). This agrees with other estimates of surface residence times of weeks to a few months [*de Baar and de Jong*, 2001; *Sarthou et al.*, 2003]. The atmospheric Fe concentrations at the winter 30°N station were very low, and the residence time calculation gave unrealistic results. This station had a well-defined surface maximum within the mixed layer, which may have been a transient, non–steady-state feature (Figure 4a).

[29] For the 24.5°S station, concurrent measurements of dust were not available. Estimates of dust deposition from *Vink and Measures* [2001] were used from a similar transect in June 1996. Because of the variability of dust dissolution, two cases (3% and 10%) were chosen on the basis of the observations from *Chen and Siefert* [2004], and residence times of 14 and 4 months were calculated respectively. The long residence time calculated for the 3% case may be due to our estimate of total atmospheric input being too low. Another possibility is that the surface residence time is longer in an area without large atmospheric input and lower surface DFe concentrations.

3.3.3. Deepwater Column Fe Profiles

[30] Deepwater DFe concentrations varied with water masses depending on their source, age, and transit pathways. Two deepwater profiles were collected at 10°N and 30°N during the winter 2001 North Atlantic cruise and one deep profile was sampled at 24.5°S on the March 2002 South Atlantic cruise. At the 10°N station, DFe values decrease to an average value of 0.73 ± 0.12 nmol/kg (1 SD, n = 3) below (>1600 m) the high DFe of the OMZ. From the salinity profile (Figures 4c and 6b), the water from 1600 m to 4200 m can be identified as North Atlantic Deep Water (NADW). The *Wu et al.* [2001] 35°N station also sampled NADW (see salinity profile, Figure 6b) and had an average value of 0.64 ± 0.05 nmol/kg (n = 6) at depths greater than 1600 m, which is lower than our observed value. However, we only have three samples below 1600 m, and the 3400-m sample yielded high DFe (0.86 nmol/kg) and hence is potentially contaminated. The concentration was measured in analyses from several filtrate bottles, so the datum is retained in the sample plots and calculations. The 30°N station was only sampled to 1050 m and did not sample NADW, but DFe increased below the pycnocline (Figure 4a).

[31] The South Atlantic water column profile Fe data are the first reported that show variations within all the major water masses in the South Atlantic. In Figure 5a, the DFe profile is shown along with reactive silicate data. Antarctic Intermediate Water (AAIW) is the high-Si water just below the pycnocline from 700 to 1200 m and has a DFe value of 0.38 ± 0.01 nmol/kg (1 SD, n = 4). NADW has lower Si concentration and forms the core of the deep water from 1700 to 3350 m with higher DFe concentrations (0.47 ± 0.02 nmol/kg, 1SD, n = 7). Below 3500 m, Si levels increase to very high levels at 4040 m (118 μmol/kg) indicative of Antarctic Bottom Water/Lower Circumpolar Deep Water (AABW/LCPDW). The DFe in the AABW/LCPDW was 0.42 ± 0.01 nmol/kg (1 SD, n = 4). There are few measurements of DFe in the Atlantic sector of the Southern Ocean, and those data are mostly from surface water. Surface waters vary from 0.1 to 0.5 nmol/kg [*Martin et al.*, 1990b; *de Baar et al.*, 1995; *Loscher et al.*, 1997], and DFe concentrations from a profile near the Drake Passage

were 0.10 to 0.16 nmol/kg at the surface and increased to 0.40 nmol/kg at 550 m [*Martin et al.*, 1990b]. These deeper Antarctic DFe concentrations are comparable with our observations of DFe concentrations for AAIW and AABW/LCPDW at our site. The higher DFe in the NADW compared to the Antarctic derived water masses is likely due to the different sources and pathways of these water masses. NADW is derived from the North Atlantic that has higher dust inputs and Fe-replete sinking organic matter. In contrast, the Antarctic derived water masses originate in a region of the ocean that has low atmospheric dust inputs and severe Fe limitation.

[32] Two qualitatively useful parameters (Fe* and AOU estimated Fe:C regeneration ratios) were estimated for the various water masses sampled in the deep water at our sites (Table 1). Fe* is defined by *Parekh et al.* [2005] and is calculated with the following formula: Fe* = [Fe] − (Fe/P)uptake ratio*[PO4−]. Fe* is a measure of the Fe deficiency of the water for biological growth with negative values indicating that there is insufficient Fe to support growth based on the available phosphate. The Fe:P uptake ratio (0.47 mmol/mol) used in this estimation corresponds to a Fe:C ratio of 4 μmol/mol [*Sunda and Huntsman*, 1995] using a Redfield C:P of 117 [*Anderson and Sarmiento*, 1994]. The Fe:C ratio used for the Fe* calculation is a reasonable value for a minimum amount of Fe needed for growth by oceanic species [*Sunda and Huntsman*, 1995].

[33] As shown in Table 1, Fe* values for the North Atlantic sites are mostly slightly positive, whereas Fe* is negative for all the water masses at the South Atlantic site. The most severe Fe deficiencies are observed in the Antarctic-derived water masses. The general pattern of Fe* agrees well with model derived estimates of Fe* by *Parekh et al.* [2005]. The NADW, a major source of water upwelling in the Southern Ocean [*Tchernia*, 1980], is already deficient in DFe relative to phosphate at 24.5°S owing to removal of Fe by scavenging (Fe* of −0.15 nmol/kg). The severe deficiency of Fe relative to phosphate in waters derived from the Southern Ocean is caused by upwelling water already being deficient in Fe as well as the low dust supply to the Southern Ocean, which does not supply enough Fe for the biological pump to utilize the entire phosphate pool. Therefore a large excess of phosphate is left in the surface waters when it sinks. The excess phosphate combined with progressive scavenging of Fe as the Antarctic water masses move north leads to the low Fe* values observed (−0.43 to −0.57 nmol/kg). It is interesting that the Fe* values in the North Atlantic are positive. This lends support to arguments by *Sunda* [1997] that sinking organic matter in the North Atlantic has higher Fe:C ratios owing to luxury uptake of Fe when more Fe is available.

[34] The other quantity estimated from our data set was Fe:C regeneration ratios based on AOU measurements and an O_2:C ratio of −1.6 [*Martin et al.*, 1987; *Sunda*, 1997]. The AOU derived Fe:C regeneration ratio represents the Fe:C ratio of remineralized organic matter, but is only valid in water masses that sank with very little preformed Fe and have not had significant loss of DFe due to scavenging (young water masses). The Fe:C ratio of 11 μmol/mol estimated for the OMZ at the 10°N site may be representative of Fe:C ratios of sinking organic matter in the North Atlantic due to the high levels of remineralized DFe in the OMZ and the relatively young age of this water. The NADW at 10°N has an elevated Fe:C regeneration ratio of ∼17 μmol/mol, which may be due to higher Fe:C ratios of sinking organic matter in the North Atlantic or preformed Fe in the NADW when it sank the in the North Atlantic. A preformed DFe of 0.3 nmol/kg would lower the estimated Fe:C regeneration ratio to ∼10 μmol/mol. At 24.5°S, the NADW Fe:C regeneration ratio decreases to 11 μmol/mol (from 17 μmol/mol in the North Atlantic) indicating net loss of Fe by scavenging. The two Antarctic derived water masses (AAIW and AABW/LCPDW) at 24.5°S have significantly lower Fe:C regeneration ratios of 5 to 7 μmol/mol, which suggest that remineralized organic matter in the South Atlantic and Southern Ocean has lower Fe:C values than the North Atlantic remineralized organic matter. The AOU-derived estimates of the Fe:C of sinking organic matter in this study indicate that this ratio may vary by up to a factor two in the Atlantic supporting arguments by *Sunda* [1997].

3.3.4. Deepwater Residence Time Estimate

[35] The DFe data set can also be used to estimate the scavenging residence time for DFe in NADW. This can be estimated from the difference between DFe in the North Atlantic sites and the South Atlantic site. The NADW at the South Atlantic site (0.47 ± 0.02 nmol/kg, 1 SD, n = 4) has significantly less DFe than the average of NADW from the northern sites (0.67 ± 0.09 nmol/kg, 1 SD, n = 9). Salinity and silicate data indicate that the NADW has not been significantly diluted with Antarctic water sources during transit from the North Atlantic to 24.5°S station. The NADW value for the North Atlantic is an average of the DFe concentrations from depths greater than 1600 m from the 10°N site from this study and the 35°N site from *Wu et al.* [2001]. Neither North Atlantic site sampled deep enough to include AABW/LCPDW (see salinity plot, Figure 6b), so all sample depths below 1600 m are included in the average. The measured difference in the DFe between the North Atlantic sites and the South Atlantic site is significant at the 95% confidence level using the t-test and a distribution-free test, the Kolmogorov-Smirnov test [*Hollander and Wolfe*, 1973].

[36] In order to calculate a scavenging residence time for the DFe in the NADW, several factors were considered including (1) dilution of the NADW with low Fe Antarctic water, (2) remineralization of organic bound Fe along the flow path, and (3) the transit time of NADW from the North Atlantic (at 10°N) to the South Atlantic site (24.5°S). As can be seen by the salinity profile (Figure 6b), the core of the NADW salinity from all sites is nearly the same indicating very little dilution of the NADW from lower salinity Antarctic water. However, if one assumes that the small increase in Si in NADW observed at GEOSECS stations near our stations (station 39: 8°N, 44°W; station 57: 24°S, 35°W) is due to dilution of low-Si NADW with high-Si Antarctic water, a modest dilution factor of 3.5% can be estimated. Dilution could then account for 0.01 nmol/kg of the DFe decrease from the North to South Atlantic assuming 0.40 nmol/kg DFe for Antarctic deep

water. DFe gain from remineralization of organic matter was calculated from the small increase in phosphate from the two GEOSECS sites after correcting the phosphate for dilution of NADW with Antarctic waters. Using a Fe:P remineralization ratio of ~1 mmol/mol (corresponds to an Fe:C of 10 μmol/mol and a C:P of 117), a regeneration input of 0.04 nmol/kg DFe can be estimated for the transit from the northern to the southern station. Combining the dilution loss and the regeneration gain, an increase of DFe of 0.03 ± 0.02 nmol/kg was estimated between the north and south stations. The uncertainty in this estimate is large because both the Fe:C regeneration ratio and the dilution factor could differ by a factor of 2. The transit time of NADW was estimated using mixing-corrected radiocarbon age estimates for western Atlantic deep water [*Broecker and Virgilio*, 1991]. Averaging multiple stations from *Broecker and Virgilio* [1991] around our 10°N and 25°S stations resulted in an age difference of ~56 ± 18 years.

[37] A scavenging residence time estimate of 270 ± 140 years was calculated for deepwater DFe based on the observed loss of DFe (0.20 nmol/kg) and the estimated input of 0.03 nmol/kg DFe from regeneration minus dilution in the transit from the northern to southern station. Changing the regenerative- and mixing-induced input to lower and higher estimates of 0.01 and 0.05 nmol/kg does not significantly change the scavenging residence time estimate (300 and 250 years, respectively). Our derived scavenging residence time is very sensitive to the observed decrease in DFe from the north to south sites and the estimated transit time (e.g., lowering the transit time to 40 years changes our estimate of scavenging residence time to 200 years). The ~50% uncertainty in our estimate is due to the uncertainties in the difference between the DFe between the North Atlantic and South Atlantic sites and the transit time. Our estimate of scavenging residence time agrees with published estimates of residence time based either on indirect methods [*Bruland et al.*, 1994] or models [*Johnson et al.*, 1997; *Parekh et al.*, 2005]. However, our estimate is longer than residence time estimations made by *de Baar and de Jong* [2001]. Their residence time calculations of less than 50 years were made using estimates of input of DFe to the deep ocean that have very large uncertainties (order of magnitude) associated with them. Our residence time estimate is based on the output of DFe (scavenging) in a water mass where transit time, input from regeneration of organic matter, and dilution loss could be constrained.

4. Conclusions

[38] In the subtropical and tropical Atlantic, surface DFe and DMn concentrations follow dust deposition trends. The coupling of dust deposition and dissolved concentrations of these elements is modified by their chemistry in the surface waters. For DFe, biological uptake and scavenging cause DFe levels to be variable and have residence times in surface waters on the order of months (1 to 5 months and possibly longer in the low DFe, low dust deposition regions of the South Atlantic). On the basis of dust solubility experiments (mesocosm incubation experiments), lower DFe compared to dissolved Al, and observed excess ligand concentrations in the North Atlantic, there may be a solubility limit to how much atmospheric Fe can dissolve in the North Atlantic surface waters (~1.15 nmol/kg). DMn has a longer residence time in surface waters (decades) due to photochemical cycling; therefore the correlation of DMn and dust deposition is eroded owing to cycling and lateral advection.

[39] Three profiles were measured for DFe in this study in the western subtropical and tropical Atlantic (30°N, 10°N, and 24.5°S), The DFe concentration profiles generally have nutrient-type profiles with lower concentrations in surface waters than in deep water, although the profiles have interesting features deviating from classic nutrient-type profiles with surface maxima, intermediate water minima and maxima, and variations clearly associated with water masses. Surface maxima in DFe were observed at all sites except 10°N in the winter. At the two subtropical gyre sites (30°N, 24.5°S), the surface maxima are followed by broad minima in the DFe within the pycnocline before DFe increases below depths greater than 700 m. The surface maxima in DFe are likely due to atmospheric deposition, but the reason for the decrease in DFe at shallow depths is less clear. There are two possible explanations for the decrease in DFe: (1) some removal mechanism for the DFe between ~30 to 80 m (i.e., scavenging and biological uptake), and/or (2) episodic atmospheric dust deposition and transient downward mixing with lower DFe water. The minima in DFe are often associated with the depth of the chlorophyll maximum. This suggests that some biological uptake or scavenging mechanism is responsible for the minima. However, transient downward mixing with low DFe water is also possible because the DFe remains low throughout the pycnocline at the subtropical gyre sites. The pycnocline water at these sites is ventilated by water masses that form at higher latitude where dust deposition is lower, and therefore potentially have lower surface DFe concentrations. In particular in the South Atlantic, this water forms in an area of very low dust deposition and low surface DFe and may be responsible for the low DFe concentrations (<0.3 nmol/kg) observed throughout the pycnocline of the South Atlantic site at 24.5°S. It is likely that the cause of the DFe minima is some combination of the mechanisms listed above.

[40] In contrast to the gyre sites, the 10°N station was located on the edge of the equatorial system and had a very shallow pycnocline (<250 m). In the winter when the mixed layer was deep, it was the only station that did not have a surface maximum in DFe. DFe increased rapidly within the shallow pycnocline to concentrations >1 nmol/kg associated with an OMZ at depths of 130 to 1050 m. The increase in DFe in the OMZ is likely due to remineralization of high Fe:C organic matter into the poorly ventilated intermediate depth waters of this region. Under the more stratified summer conditions, the 10°N station had a surface maximum followed by a minimum from 50 to 100 m.

[41] Deepwater DFe concentrations varied with water masses depending on their source, age, and transit pathways. DFe concentrations in NADW decrease by 30% from the North Atlantic to South Atlantic, but DFe in the NADW is still higher than DFe in the Antarctic derived water

masses at 24.5°S. DFe in AAIW and AABW/LCPDW is low (~0.4 nmol/kg), which is consistent with observations of DFe in the Southern Ocean. A deepwater scavenging residence time for DFe of 270 ± 140 years was estimated from the observed DFe decrease in NADW from the North Atlantic to South Atlantic sites. The deep profiles in this study support the hypothesis that deepwater concentrations of DFe are controlled by a balance between input of dissolved iron in the deep water (both from remineralization and lateral transport) and removal by scavenging. Therefore DFe varies in the deep ocean. Also it is likely that the Fe:C ratio of exported organic matter is higher (>10 μmol/mol) in the Fe replete regions of the North Atlantic than in the water masses formed in the lower DFe regions of the South Atlantic and Southern Ocean (<7 μmol/mol), which is consistent with previous estimates that this ratio may vary by a factor of 2 [*Sunda*, 1997].

[42] **Acknowledgments.** This research was supported by NSF grants OCE-0002273 and OCE-99871442. B. Bergquist was funded by the National Physical Science Foundation, Lawrence Livermore National Laboratory, and the Education Office of Woods Hole Oceanographic Institution. We thank Richard Kayser for all his efforts preparing and maintaining MITESS, and M. Reuer and A. Lima for nutrient analysis on the March 2002 cruise. We would also like to thank our colleagues in the MANTRA Biocomplexity project (A. Michaels et al.) for all their help at sea and useful discussions. Special thanks go to M. Neumann and M. Erickson for assisting in MITESS deployment and recovery at sea, to Ron Siefert and Ying Chen for aerosol collection and analysis, and to Douglas Capone and coworkers for running the large volume mesocosm experiments. We thank the officers and crews of the R/V *Knorr*, R/V *Seward Johnson*, and R/V *Endeavor*.

References

Anderson, L., and J. Sarmiento (1994), Redfield ratios of remineralization determined by nutrient data analysis, *Global Biogeochem. Cycles*, *8*, 65–80.

Archer, D. E., and K. Johnson (2000), A model of the iron cycle in the ocean, *Global Biogeochem. Cycles*, *14*, 269–279.

Bell, J., J. Betts, and E. A. Boyle (2002), MITESS: A moored in-situ trace element serial sampler for deep-sea moorings, *Deep Sea Res., Part I*, *49*, 2103–2118.

Bergquist, B. A. (2004), The marine geochemistry of iron and iron isotopes, Ph.D. thesis, Mass. Inst. of Technol. and Woods Hole Oceanogr. Inst. Joint Program in Oceanogr., Cambridge, Mass.

Boyd, P. W., et al. (2000), A mesoscale phytoplankton bloom in the polar Southern Ocean stimulated by iron fertilization, *Nature*, *407*, 695–702.

Boyd, P. W., et al. (2004), The decline and fate of an iron-induced subarctic phytoplankton bloom, *Nature*, *428*, 549–553.

Boyle, E. A. (1997), What controls dissolved iron concentrations in the world ocean—A comment, *Mar. Chem.*, *57*, 163–167.

Boyle, E. A., B. A. Bergquist, R. Kayser, and N. Mahowald (2005), Iron, manganese, and lead at Hawaii Ocean Time Series Station ALOHA: Temporal variability and an intermediate water hydrothermal plum, *Geochim. Cosmochim. Acta*, *69*, 933–952.

Broecker, W. S., and A. Virgilio (1991), Radiocarbon age of waters in the deep Atlantic revisited, *Geophys. Res. Lett.*, *18*(1), 1–3.

Bruland, K. W., K. J. Orians, and J. P. Cowen (1994), Reactive trace metals in the stratified central North Pacific, *Geochim. Cosmochim. Acta*, *58*, 3171–3182.

Chen, Y., and R. Siefert (2004), Seasonal and spatial distributions of dry deposition fluxes of atmospheric total and labile iron over the tropical and sub-tropical North Atlantic Ocean, *J. Geophys. Res.*, *109*, D09305, doi:10.1029/2003JD003958.

Chiapello, I., G. Bergametti, L. Gomes, B. Chatenet, F. Dulac, J. Pimenta, and E. S. Soares (1995), An additional low layer transport of Shaelian and Saharan dust of the northeastern tropical Atlantic, *Geophys. Res. Lett.*, *22*(23), 3191–3194.

Coale, K. H., et al. (1996), A massive phytoplankton bloom induced by an ecosystem-scale iron fertilization experiment in the equatorial Pacific Ocean, *Nature*, *383*, 495–501.

Coale, K. H., et al. (2004), Southern ocean iron enrichment experiment: Carbon cycling in high- and low-Si waters, *Science*, *304*(5669), 408–414.

de Baar, H. J. W., and J. T. M. de Jong (2001), Distributions, sources and sinks of iron in seawater, in *The Biogeochemistry of Iron in Seawater*, edited by K. A. Hunter and D. Turner, pp. 123–253, John Wiley, Hoboken, N. J.

de Baar, H. J. W., J. T. M. de Jong, D. C. E. Bakker, B. M. Loscher, C. Veth, U. Bathmann, and V. Smetacek (1995), The importance of iron for plankton blooms and carbon dioxide drawdown in the Southern Ocean, *Nature*, *373*, 412–415.

de Baar, H. J. W., J. T. M. de Jong, R. F. Notling, K. R. Timmermans, M. A. van Leeuwe, U. Bathmann, M. R. van der Loeff, and J. Sildman (1999), Low dissolved Fe and the absence of diatom blooms in the remote Pacific waters of the Southern Ocean, *Mar. Chem.*, *66*, 1–34.

Duce, R. A., and N. W. Tindale (1991), Atmospheric transport of iron and its deposition in the ocean, *Limnol. Oceanogr.*, *36*, 1715–1726.

Falkowski, P. G. (1998), Evolution of the nitrogen cycle and its influence on the biological sequestration of CO2 in the ocean, *Nature*, *387*, 272–275.

Fukumori, I., F. Martel, and C. Wunsch (1991), The hydrography of the North-Atlantic in the early 1980s—An atlas, *Prog. Oceanogr.*, *27*, 1–110.

Fung, I. Y., S. K. Meyn, I. Tegen, S. C. Doney, J. G. John, and K. B. Bishop (2000), Iron supply and demand in the upper ocean, *Global Biogeochem. Cycles*, *14*, 281–295.

Gao, Y., Y. J. Kaufman, D. Tanre, D. Kolber, and P. G. Falkowski (2001), Seasonal distributions of aeolian iron fluxes to the global ocean, *Geophys. Res. Lett.*, *28*(1), 29–32.

Gledhill, M., and C. M. G. van den Berg (1994), Determination of complexation of iron (III) with natural organic complexing ligands in seawater using cathodic stripping voltammetry, *Mar. Chem.*, *47*, 41–54.

Gregg, W. W., P. Ginoux, P. S. Schopf, and N. W. Casey (2003), Phytoplankton and iron: Validation of a global three-dimensional ocean biogeochemical model, *Deep Sea Res., Part II*, *50*, 3143–3169.

Hollander, M., and D. A. Wolfe (1973), *Nonparametric Statistical Methods*, John Wiley, Hoboken, N. J.

Husar, R. B., J. M. Prospero, and L. L. Stowe (1997), Characterization of tropospheric aerosols over the oceans with the NOAA advanced very high resolution radiometer optical thickness operational product, *J. Geophys. Res.*, *102*, 16,889–16,909.

Hutchins, D. A., and K. W. Bruland (1998), Iron-limited diatom growth and Si:N uptake ratios in a coastal upwelling regime, *Nature*, *393*, 561–564.

Jickells, T. D., and L. J. Spokes (2001), Atmospheric iron inputs to the oceans, in *The Biogeochemistry of Iron in Seawater*, edited by K. A. Hunter and D. Turner, pp. 85–121, John Wiley, Hoboken, N. J.

Johnson, K. S., R. M. Gordon, and K. H. Coale (1997), What controls dissolved iron concentrations in the world ocean, *Mar. Chem.*, *57*, 137–161.

Johnson, K. S., et al. (2003), Surface ocean–lower atmosphere interactions in the northeast Pacific Ocean gyre: Aerosols, iron, and the ecosystem response, *Global Biogeochem. Cycles*, *17*(2), 1063, doi:10.1029/2002GB002004.

Klinkhammer, G. P., and M. L. Bender (1980), The distribution of manganese in the Pacific Ocean, *Earth Planet. Sci. Lett.*, *46*, 361–384.

Kumar, N., R. F. Anderson, R. A. Mortlock, P. N. Froelich, P. Kubik, B. Dittrich-Hannon, and M. Suter (1995), Increased biological productivity and export production in the glacial Southern Ocean, *Nature*, *378*, 675–680.

Landing, W. M., and K. W. Bruland (1980), Manganese in the North Pacific, *Earth Planet. Sci. Lett.*, *49*, 45–56.

Landing, W. M., and K. W. Bruland (1987), The contrasting biogeochemistry of iron and manganese in the Pacific Ocean, *Geochim. Cosmochim. Acta*, *51*, 29–43.

Landing, W. M., C. I. Measures, C. S. Buck, and M. Brown (2003), Sections of dissolved iron and aluminum from the 2003 repeat hydrography A16N expedition, *Eos Trans. AGU*, *84*(52), Ocean Sci. Meet. Suppl., Abstract OS31L-07.

Lefevre, N., and A. J. Watson (1999), Modeling the geochemical cycle of iron in the oceans and its impact on atmospheric CO_2 concentrations, *Global Biogeochem. Cycles*, *13*, 727–736.

Loscher, B. M., H. J. W. de Baar, J. T. M. de Jong, C. Veth, and F. Dehairs (1997), The distribution of Fe in the Antarctic circumpolar current, *Deep Sea Res., Part II*, *44*, 143–187.

Luther, G. W. I., and J. Wu (1997), What controls dissolved iron concentrations in the world ocean?—A comment, *Mar. Chem.*, *57*, 173–179.

Mahowald, N., K. Kohfeld, M. Hansson, Y. Balkanski, S. P. Harrison, I. C. Prentice, M. Schulz, and H. Rodhe (1999), Dust sources and deposition

during the Last Glacial Maximum and current climate: A comparison of model results with paleodata from ice cores and marine sediments, *J. Geophys. Res.*, *104*, 15,895–15,916.

Martin, J. H. (1990), Glacial-interglacial CO_2 change: The iron hypothesis, *Paleoceanography*, *5*, 1–13.

Martin, J. H., and S. E. Fitzwater (1988), Iron deficiency limits phytoplankton growth in the north-east Pacific subarctic, *Nature*, *331*, 341–343.

Martin, J. H., G. A. Knauer, D. M. Karl, and W. W. Broenkow (1987), VERTEX: Carbon cycling in the northeast Pacific, *Deep Sea Res.*, *34*, 267–285.

Martin, J. H., S. E. Fitzwater, and R. M. Gordon (1990a), Iron deficiency limits phytoplankton growth in Antarctic waters, *Global Biogeochem. Cycles*, *4*, 5–12.

Martin, J. H., R. M. Gordon, and S. E. Fitzwater (1990b), Iron in Antarctic waters, *Nature*, *345*, 156–158.

Martin, J. H., et al. (1994), Testing the iron hypothesis in ecosystems of the equatorial Pacific Ocean, *Nature*, *371*, 123–129.

Measures, C. I., and E. T. Brown (1996), Estimating dust input to the Atlantic Ocean using surface water Al concentrations, in *The Impact of African Dust Across the Mediterranean*, edited by S. Guerzoni and R. Chester, 389 pp., Springer, New York.

Measures, C. I., and S. Vink (2000), On the use of dissolved aluminum in surface waters to estimate dust deposition to the ocean, *Global Biogeochem. Cycles*, *14*, 317–327.

Moulin, C., C. E. Lambert, F. Dulac, and U. Dayan (1997), Control of the atmospheric export of dust from North Africa by the North Atlantic Oscillation, *Nature*, *387*, 691–694.

Orians, K. J., and K. W. Bruland (1986), The biogeochemistry of aluminum in the Pacific Ocean, *Earth Planet. Sci. Lett.*, *78*, 397–410.

Parekh, P., M. J. Follows, and E. A. Boyle (2005), Decoupling of iron and phosphate in the global ocean, *Global Biogeochem. Cycles*, *19*, GB2020, doi:10.1029/2004GB002280.

Powell, R., and J. Donat (2001), Organic complexation and speciation of iron in the South and equatorial Atlantic, *Deep Sea Res., Part II*, *48*, 2877–2893.

Prospero, J. M. (1996), The atmospheric transport of particles to the ocean, in *Particle Flux in the Ocean*, edited by V. Ittekkott et al., pp. 19–52, John Wiley, Hoboken, N. J.

Rue, E. L., and K. W. Bruland (1995), Complexation of iron (III) by natural ligands in the central North Pacific as determined by a new competitive ligand equilibrium/adsorptive cathodic stripping voltammetric method, *Mar. Chem.*, *50*, 117–138.

Rueter, J. G., and D. R. Ades (1987), The role of iron nutrition in photosynthesis and nitrogen assimilation in Scenedesmus quadeicauda (Chlorophyceae), *J. Phycol.*, *23*, 452–457.

Sarthou, G., et al. (2003), Atmospheric iron deposition and sea-surface dissolved iron concentrations in the eastern Atlantic Ocean, *Deep Sea Res., Part I*, *50*, 1339–1352.

Sigman, D. M., and E. A. Boyle (2000), Glacial/Interglacial variations in atmospheric carbon dioxide: Searching for a cause, *Nature*, *407*, 859–868.

Sunda, W. G. (1997), Control of dissolved iron concentrations in the world ocean: A comment, *Mar. Chem.*, *57*, 169–172.

Sunda, W. G., and S. A. Huntsman (1988), Effects of sunlight on redox cycles of manganese in the southwestern Sargasso Sea, *Deep Sea Res.*, *35*, 1297–1317.

Sunda, W. G., and S. A. Huntsman (1995), Iron uptake and growth limitation in oceanic and coastal phytoplankton, *Mar. Chem.*, *50*, 189–206.

Tchernia, P. (1980), *Descriptive Regional Oceanography*, 253 pp., Elsevier, New York.

Vink, S., and C. I. Measures (2001), The role of dust deposition in determining surface water distributions of Al and Fe in the south west Atlantic, *Deep Sea Res., Part II*, *48*, 2787–2809.

Wedepohl, K. H. (1995), The composition of the continental crust, *Geochim. Cosmochim. Acta*, *59*, 1217–1232.

Wells, M. L., N. M. Price, and K. W. Bruland (1995), Iron chemistry in seawater and its relationship to phytoplankton, *Mar. Chem.*, *48*, 157–182.

Witter, A. E., and G. W. Luther (1998), Variation in Fe-organic complexation with depth in the northwestern Atlantic Ocean as determined using a kinetic approach, *Mar. Chem.*, *62*, 241–258.

Wu, J., and E. A. Boyle (1998), Determination of iron in seawater by high resolution inductively coupled plasma mass spectrometry after Mg (OH)2 coprecipitation, *Anal. Chim. Acta*, *367*, 183–191.

Wu, J., and E. A. Boyle (2002), Iron in the Sargasso Sea: Implications for the processes controlling dissolved Fe distribution in the ocean, *Global Biogeochem. Cycles*, *16*(4), 1086, doi:10.1029/2001GB001453.

Wu, J., and G. W. Luther (1995), Complexation of iron (III) by natural organic ligands in the northwest Atlantic Ocean by competitive ligand equilibration method and a kinetic approach, *Mar. Chem.*, *50*, 159–177.

Wu, J., and G. W. Luther (1996), Spatial and temporal distribution of iron in surface water of the northwest Atlantic Ocean, *Geochim. Cosmochim. Acta*, *60*, 2729–2741.

Wu, J., E. A. Boyle, W. Sunda, and L. Wen (2001), Soluble and colloidal iron in the oligotrophic North Atlantic and North Pacific, *Science*, *293*, 847–849.

B. A. Bergquist, Department of Geological Sciences, University of Michigan, 2534 C.C. Little Building, 1100 North University Avenue, Ann Arbor, MI 48109, USA. (bbergqui@umich.edu)

E. A. Boyle, Earth, Atmospheric, and Planetary Sciences, Massachusetts Institute of Technology, Cambridge, MA 02139, USA.